The Use Dielectric-Coated Metal Hollow Fiber for Terahertz Wave metal Underground Sensors

WANG Ke-jia [1], WANG Qi [1], WANG Yi [2], ZHANG Shuai [3]
(1 Electrical Engineering and Automation School of Harbin Institute of Technology ,Harbin 150001,P.R.China
2 Information Engineering College of China Jiliang University
3 Information and Communication Engineering College of Harbin Engineering University)

Abstract Transmission characteristics and mode structure of both metal hollow fiber and dielectric-coated metal hollow fiber for terahertz wave are studied. Theoretical evaluation shows that the TE11mode is dominant in metal hollow fiber and has high coupling efficiency when a linearly polarized light source is launched. HE11mode is mainly supported in dielectric-coated metal hollow fiber with an optimum thickness for the dielectric film. The transmission loss of the TE11and HE11mode is8.4dB/m and 2dB/m respectively at the wavelength of 200μm for the hollow fibers with 1mm bore size. The effects of optical constants of metals and dielectric materials on attenuation coefficient are also discussed to optimize the transmission performance of dielectric-coated metal hollow fiber.Aluminum is the best choice among the commonly-used metals based on published optical constants. The optimum value for the refractive index of the dielectric film is1.41. According to the primary measuring results, polyethylene is a proper choice as its refractive index is1.51and it brings low absorption in terahertz waves.

The use of Dielectric-Coated Metal Hollow Fiber Bragg phase-shifted fiber grating, for optical fiber and metal combine downhole drill pipe deformation temperature and strain detection underground. Phase-Shifted Fiber Bragg Grating using photoelectric heterodyne detection frequency, the frequency range up to 10^{12}Hz, the frequency resolution of 1KHz. LPFG, photovoltaic devices and microwave heterodyne frequency meter combination can solve the phase-shift grating sensor speed and resolution issues.

Key words optical waveguide; terahertz hollow fiber; mode structure; transmission sensor

1. INTRODUCTION

In the field of mine detection, the metallic hollow optical waveguides and metallic hollow fiber grating sensing, transmission method are used to study key problems about transmission theory and technique of logging signal wideband, high-speed, anti-environmental impact, ability against strong interference [1][2] . So that information transmission optical fiber laser sensor moves toward the new practical application in the logging. This article studies low-loss air-core transmission channel theory of the metallic hollow optical fiber, coherent reception method and information fusion. The coherent optical information communication and testing method for overcoming the effect of the bad work environment on BER (Bit Error Rate) is used. Dielectric-coated metal fiber in the drill pipe works under special conditions (rotation, multi-connection) for Terahertz wave, the effect of metal and quartz optical waveguide changes on signal attenuation [3] . As a result of large signal attenuation and uncertainty, the use of photoelectric detection is to be necessary, the loss of optical power can be compensated by optical power in local oscillator.

Based on the two-layered structure, a sensitive thin film outside the fiber grating clad to constitute three-layered structure LPFG [1][2], LPFG cladding mode will be more sensitive to changes in refractive index, may manufacture a variety of sensors. This article based on the coupled-mode equation, uses the transmission matrix method on cascaded LPFG. The effects of the length, position of the fiber that connects the LPFG on the transmission spectrum of the cascaded LPFG were discussed. The high sensitivity examination which through optoelectronic heterodyne detection on the three-layered cascaded LPFG's transmission spectrum migration, may constitute chemistry, mechanics, the

International Symposium on Photoelectronic Detection and Imaging 2009: Terahertz and High Energy Radiation Detection Technologies and Applications, edited by X.-C. Zhang, James M. Ryan, Cun-lin Zhang, Chuan-xiang Tang, Proc. of SPIE Vol. 7385, 738522 · © 2009 SPIE · CCC code: 0277-786X/09/$18 · doi: 10.1117/12.836001

electricity[10][11], the optics precision sensor. The high sensitivity examination which through optoelectronic heterodyne detection on the three-layered cascaded LPFG's transmission spectrum migration, may constitute precision sensor on the Underground.

2. THEORETICAL ANALYSIS

2.1 Dielectric-coated metal fiber grating sensors

1) Dielectric-Coated Metal Fiber

Underground sensors must be used high-strength metal hollow optical fiber, which frequency is in the THz. Underground metallic hollow optical fiber sensor can be divided into four categories:

① the metallic hollow optical fiber [4][5], optical fiber wall rough, transmission loss is big, and short-distance transmission is THz wave (centimeter level)

②The carbon fiber dielectric-coated metal hollow optical fiber media[6], loss is small, the flexibility is good, but the curving loss are big.

③Carbon hollow fiber tube within metal film, the metallic hollow optical fiber support TE11 mode in the THz transmission. The metallic hollow optical fiber[7][8], when inside diameter is 3mm, in the wave length 158.31μm loss is 3.9 dB/m, and inside diameter is 1mm, in the wave length 190~250μm loss is 7.5~8.0 dB/m. Experimental measurement shows that when the optical fiber to a radius of 15 cm for 90 ° bending, the additional loss is less than 0.5 dB.

④Carbon hollow fiber tube within dielectric film and metal film, that is Dielectric-Coated Metal Hollow Fiber.

Dielectric film increases the reflectivity of metal surface, greatly reduced the transmission loss. Silver Polystyrene Hollow fiber, which reduced the transmission loss greatly when the polystyrene (PE) gets the optimal value of thickness. The fiber-optic transmission supports the HE11 mode. The loss of Silver polystyrene Hollow fiber with Diameter of 2 mm, length 90 cm is 0.95 dB /m in 119μm, which is most suitable for underground fiber-optic materials in long-distance fiber-optic sensor[9].

2) Metal fiber grating

In the while drilling logging broadband signal transmission, through the metallic hollow optical waveguides theory and metallic hollow fiber grating sensing, transmission method are used to study key problems about transmission theory and technique of logging signal wideband, high-speed, anti-environmental impact. It's necessary to use fiber grating sensor.

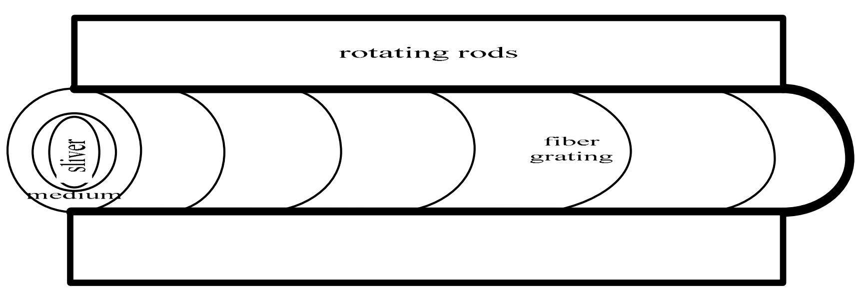

Fig.1 Silver-plating dielectric hollow fiber schematic drawing

Metal optical fiber may use two kinds of grating.

 Phase-shift grating

Phase-shift grating is a non-uniform grating, Figure 2 (a) shows that FBG structural sketch map. In order to analyze reflective properties and transmission characteristics, it's deduced based on coupled mode theory and the transfer matrix method.

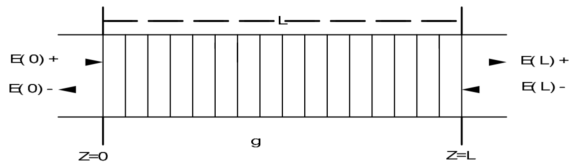

Fig 2(a) FBG structural sketch map

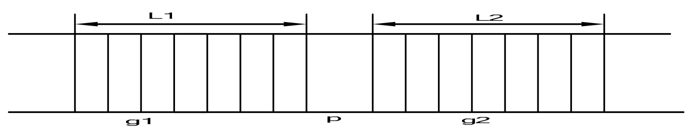

Fig 2(a) Phase-shift FBG structural sketch map

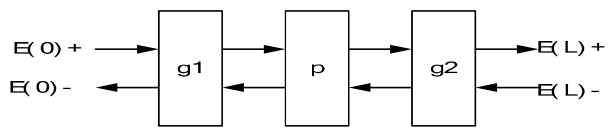

Fig 2(a) FBG transmission sketch map

$E^{+}(0)$, $E^{+}(L)$, $E^{-}(0)$ and $E^{-}(L)$ is forward and back transmission light wave field intensity in the point of 0 and L. L is the grating length. When its equivalent is four pole mouth apparatus, according to the coupled mode transmission theory, the both sides E^{+}, E^{-} of FBG may express as transmission matrix

$$\begin{bmatrix} E^{+}(0) \\ E^{-}(0) \end{bmatrix} = [g] \cdot \begin{bmatrix} E^{+}(L) \\ E^{-}(L) \end{bmatrix} = \begin{bmatrix} m & n \\ n^{*} & m^{*} \end{bmatrix} \cdot \begin{bmatrix} E^{+}(L) \\ E^{-}(L) \end{bmatrix} \tag{1}$$

The value of matrix elements is obtained by the coupled-mode theory

$$m = \cosh(\alpha L) - i\sigma \sinh(\alpha L)/\alpha \tag{2}$$

$$n = -ik \sinh(\alpha L)/\alpha \tag{3}$$

Where * denotes conjugate complex, $\alpha^2 = k^2 - \sigma^2, k = \pi \Delta n / \lambda_B$ is the grating coupling coefficient; $\sigma = 2\pi n_{eff}(\lambda^{-1} - \lambda_B^{-1})$ offset of Bragg wavelength, $\lambda_B - 2n_{eff}\Lambda$ is Bragg wavelength, Λ is grating period, n_{eff} is the effective refractive index of optical fiber, Δn is refractive index modulation depth. The reflection coefficient r of FBG can be get from boundary condition $E^{-}(L) = 0$.

$$r = \frac{E^{-}(0)}{E^{+}(0)} = \frac{n^{*}}{m} = \frac{-k \sinh(\alpha L)}{\sigma \sinh(\alpha L) + i\alpha \cosh(\alpha L)} \tag{4}$$

Phase-shift grating with only one phase mutation may regard as cascaded by the two sub-grating cascade. The light wave field's phase between two sub-gratings has a sudden change. Its structural sketch map is shown in Figure 2(b). g1, g2, p is the even sub-gratings grating and phase shift. Figure 2 (c) is the transfer matrix model. When phase-shift is j, the phase shift of the matrix can be expressed as

$$[p]=\begin{bmatrix} e^{-j\varphi} 0 \\ 0 \quad e^{j\varphi} \end{bmatrix} \tag{5}$$

Sub-paragraph grating and phase shift can be multiplied by the matrix phase-shift grating transfer equation

$$\begin{bmatrix} E^{+}(0) \\ E^{-}(0) \end{bmatrix} = \begin{bmatrix} AB \\ CD \end{bmatrix} \cdot \begin{bmatrix} E^{+}(L) \\ E^{-}(L) \end{bmatrix} \tag{6}$$

Where $\begin{bmatrix} AB \\ CD \end{bmatrix} = |g1| \cdot |p| \cdot |g2|$ (7)

Where L is the total length of phase shift grating, phase-shift grating reflection coefficient can be obtained by the introduction of boundary conditions.

$$r = \frac{E^{-}(0)}{E^{+}(0)} = \frac{C}{A} \tag{8}$$

Characteristic analysis

The Bragg wave lengths of two sub-gratings is λ_B, the coupling coefficient is k, the refractive index modulation depth is Δn, length respectively is L_1, L_2, the value of phase mutation is L_1, L_2.The above mentioned parameter is substituted in the formula (8), then the reflection coefficient of phase-shift grating light field amplitude.

$$r = \frac{jk\{[\alpha\cosh(\alpha L_2) - i\sigma\sinh(\alpha L_2)]\cdot\sinh(\alpha L_1) + [\alpha\cosh(\alpha L_1) + i\sigma\sinh(\alpha L_1)]\sinh(\alpha L_2)e^{i2p}\}}{[\alpha\cosh(\alpha L_1) - i\sigma\sinh(\alpha L_1)][\alpha\cosh(\alpha L_2) + i\sigma\sinh(\alpha L_2)] + k^2\sinh(\alpha L_1) + k^2\sinh(\alpha L_1)\cdot\sinh(\alpha L_2)e^{i2p}} \tag{9}$$

When any one of the three parameters takes zero, it becomes single stage even grating expression in the formula (9). When $L_1 = L_2$ and $\varphi = \pi/2$, there is a very narrow line width of the transmission peak, in the middle of grating stop-band, transmission wavelength is equal to the Bragg wavelength, the amplitude of transmission peak closes to 100%, resulting in the transmission peak, the grating reflection bandwidth broadening, and the peak of reflectance declined; Figure3 (a) shows reflection spectrum about before the introduction of phase shift (dashed line) and after the introduction of phase shift (real line). When $L_1 = L_2$ and $\varphi = 2\pi/5$, grating reflection spectrum curve of real line is showed in Figure 3.6; we can see transmission peak wavelength is greater than the Bragg wavelength. When $\varphi = 6\pi/5$, grating reflection spectrum curve of dashed line is showed in Figure 3(b); we can see transmission peak wavelength is less than the Bragg wavelength. Therefore the transmission peak in the grating reflection spectrum depends on phase-shift quantity. When the phase shift is in the one-tenth of grating, grating reflection spectrum curve of real line is showed in Figure 3 (c), as can be seen from the figure, the magnitude of the transmission peak depends on the phase shift in the location of the grating[11]. When $L_1 = L_2 = L$, phase-shift grating reflectivity for the light intensity is obtained by (9)

$$R = |r|^2 = \frac{4k^2\sigma^2\sinh^4(\alpha L)}{(\sigma^2 - k^2)^2 + 4k^2\sigma^2\sinh^4(\alpha L)} \tag{10}$$

The transmission peak line width is derived by the above equation, it satisfies the following equation

$$\sigma^2 - 2k\sigma\sinh^2(\alpha L) = k^2 \quad (11) \tag{11}$$

When $\sigma \approx 0$, $\alpha \approx k$, so $\sigma_h = k[\sqrt{\sinh^4(kL)+1} - \sinh^2(kL)] = k/2\sinh^2(kL)$ (12)

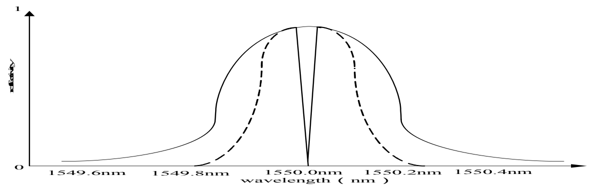

Fig 3(a) Phase shift front (dashed line) and after (real line) gratings reflection spectrum

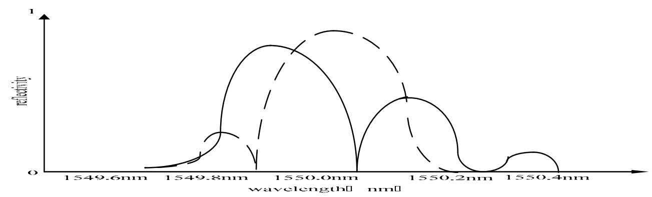

Fig 3(b) Phase shift quantity $\varphi = 2\pi / 5$ (real line) and $\varphi = 6\pi / 5$ (dashed) gratings reflection spectrum

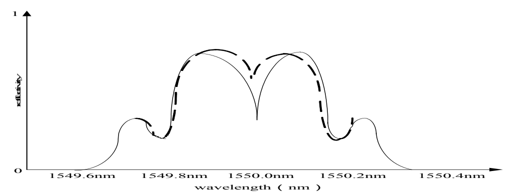

Fig 3(c) $\varphi = \pi / 2$, phase shift section $1/5\ L$ (dashed) and $1/10\ L$ (real line) reflection spectrum

The relationship between offset of Bragg wavelength and coupling coefficient

In the formula (12), when the grating length L is decided, σ_h is proportional to k and is inversely proportional to e^{2kL} . As a result, the transmission peak line width will decrease with the coupling coefficient increasing. When the coupling coefficient k is decided[12], σ_h is inversely proportional to e^{2kL} . As a result, the transmission peak line width will decrease with the coupling coefficient increasing.

The most interest is phase shift for Phase shift grating in practice. Phase shift grating can open a very narrow line width of the transmission window, because of that, it has been an important application in the strain sensor system.

The location of transmission peak in the grating reflection spectrum depends on phase shift. The amplitude of transmission peak depends on the phase shift zone position in the grating. Transmission peak line width drastically decreases with grating length and the coupling coefficient increasing, so the transmission peaks can be very narrow. At present foreign country already can manufacture phase-shift grating that the transmission peak the line width is smaller than the 1pm, comparing to ordinary reflection FBG 0.2nm, bandwidth enhances three orders of magnitude. This extremely narrow line width and controllable optical filter has an important application in the optical signal processing, such as the laser signal separation, laser wavelength division multiplexing, laser communications interference light filter and can be constructed differential phase-shift fiber optic grating for optical heterodyne processing.

Long-period grating phase shift

Phase-shift LPFG may regard as the combination of two long-period grating (LPFGI and LPFG2) separated by the length d cascaded optical fiber and the size φ of initial phase-shift. Its transmission characteristics T are as follows

$$\begin{bmatrix} t \\ r \end{bmatrix} = \begin{bmatrix} t_2 \, r_2 \\ r_2 \, t_2^* \end{bmatrix} \times \begin{bmatrix} \exp[i\pi(n_{eff}^{co} - n_{eff}^{cl})d/\lambda)0 & \\ 0 & \exp[-i\pi(n_{eff}^{co} - n_{eff}^{cl})d/\lambda] \end{bmatrix} \times$$

$$\begin{bmatrix} \exp(i\varphi/2)0 & \\ 0 & \exp(-i\varphi/2) \end{bmatrix} \times \begin{bmatrix} t_1 \, r_1 \\ r_1 \, t_1^* \end{bmatrix} \times \begin{bmatrix} 1 \\ 0 \end{bmatrix} \tag{13}$$

Where t is specific order cladding mode order transmission amplitude of the cascaded long period grating specific, r is the transmission amplitude of core mode, t_1, r_1, t_2, r_2 express separately about the amplitude of LPFG specific order cladding mode and core mode, which can be calculated according to the transmission matrix method, the even LPFG transmission matrix may be expressed as[13]

$$\begin{bmatrix} t \, r \\ rt^\bullet \end{bmatrix} = \begin{bmatrix} \cos(\gamma L) + i(\sigma/\gamma)\sin(\gamma L) i(k/\gamma)\sin(\gamma L) & \\ i(k/\gamma)\sin(\gamma L) & \cos(\gamma \Delta z) - i(\sigma/\gamma)\sin(\gamma L) \end{bmatrix} \tag{14}$$

Self-coupled coefficient is $\hat{\sigma} = \delta + \dfrac{\sigma_{11} - \sigma_{22}}{2} - \dfrac{1}{2}\dfrac{d\phi}{dz}$ (15)

Where σ_{11}, σ_{22} is DC coupling coefficient, δ is demodulation parameters, $\gamma = \sqrt{\hat{\sigma}^2 + k^2}$ (16)

By the formula (14) and long-period fiber grating parallel transmission rate formula $T = |t|^2$, we can get long-period fiber grating parallel transmission rate T. That is

$$T = \left| \exp\{i\left[2\pi\left(n_{eff}^{co} - n_{eff}^{cl}\right)d/\lambda + \varphi\right]\} t_1 t_2 + r_1 r_2 \right|^2 \tag{17}$$

2.2 Fiber-optic sensor structure and signal demodulation method

1) differential structure and coherent demodulation

Strain sensors for underground should use differential structure.

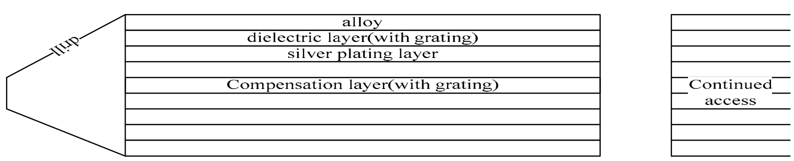

Fig. 4(a) Reflective metal fiber grating sensors structure map

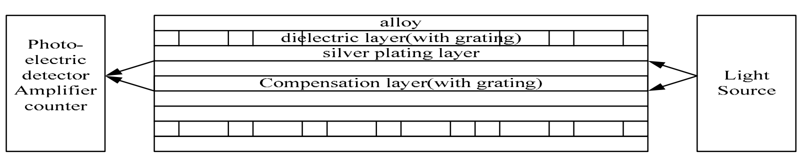

Fig. 4(b) Transmission metal fiber grating sensors structure map

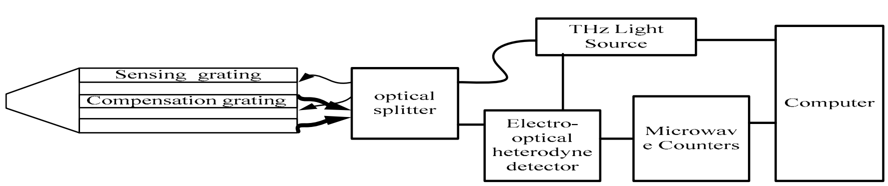

Fig. 5 Metal Fiber Grating differential sensor structure map

2) Differential fiber phase-shift grating optical heterodyne sensing technology in the application

Fiber grating uses optical heterodyne, antithetic formula phase-shift optical grating composes laser optical heterodyne system with Fiber. Wide spectrum SLD issues wide spectrum light into two pairs of antithetic formula phase-shift optical fiber grating that bonded to strain structure in tuner, the strain causes b an extension of a fiber grating compression and compression of the other. The wide-spectrum light of SLD through antithetic formula phase-shift optical grating, forms t the frequency high and low differential motion, and forms ultra-high frequency heterodyne signal, measures the frequency after the frequency count or spectral analysis through the ultra-high frequency spectrometer, which is showed in Figure (5)

Antithetic formula phase-shift grating, based on cantilever grating theory, the phase-shift grating can open the narrow-band transmission window to spectral characteristics. Phase-shift has the advantages of high-quality fiber grating wavelength selectivity, low insertion loss and has nothing to do with polarization. The transmission characteristics of single point phase shift of fiber grating: The transmission characteristics according to phase-shift size.First consider one kind of standard condition. There is only a single phase-shift in the phase transition point $z = L/2$ and suppose fiber effective refractive index $\eta = 1.46$, grating cycle $\Lambda = 531nm$, (k is the grating coupling coefficient), wavelength $\lambda = 1550nm$, strain $\delta = 2.0 \times 10^{-3}$ and grating length $L = 1mm$.

When phase transition point is $z = L/2$, phase shift is $\varphi = 0^0$, the transmission characteristics is shown in Figure 6 (a) . It is the same as the general fiber grating. When phase shift is $\varphi = 90^0$, its transmission characteristic is showed in Figure 6 (b). It is different from general fiber Bragg grating transmission characteristics, which can open a narrow transmission peak in stop band with wavelength $\lambda = 1550nm$, the bandwidth of the window is about 0.7 × 10, can be used as demultiplexer of multi-channel communication system, that is, the signal of the multi-channel system is in the grating stop-band range, there is only one channel signal can go through the grating. When phase shift is $\varphi = 45^0$, its transmission characteristic is showed in Figure 6 (c). When phase shift is $\varphi = 135^0$, its transmission characteristic is showed in Figure 6 (d).

Compare Fig 6 (c) with Figure 6 (d), we can see that the transmission spectrum is symmetrical as $\lambda = 1550nm$, resulting in migration pass band window. If the cantilever loads, then the two phase-shift fiber gratings which are fixed change in the phase shift in the opposite direction. One projection grating frequency changes in one direction, while the frequency of the other grating changes to the other direction, the difference frequency signal in the photoelectric detector is from DC to dozens of GHz. Because the optical fiber is easy to satisfy the condition that the two fiber-optic grating light output power E_1^2 E_2^2 , and the angle ϕ between polarization direction and the width $\Delta\omega$ is constant, we can detect frequency response function from the spectrum analyzer. And measure accurately difference frequency through frequency meter. We can obtain the frequency response of optoelectronic devices and the inserting optical devices.

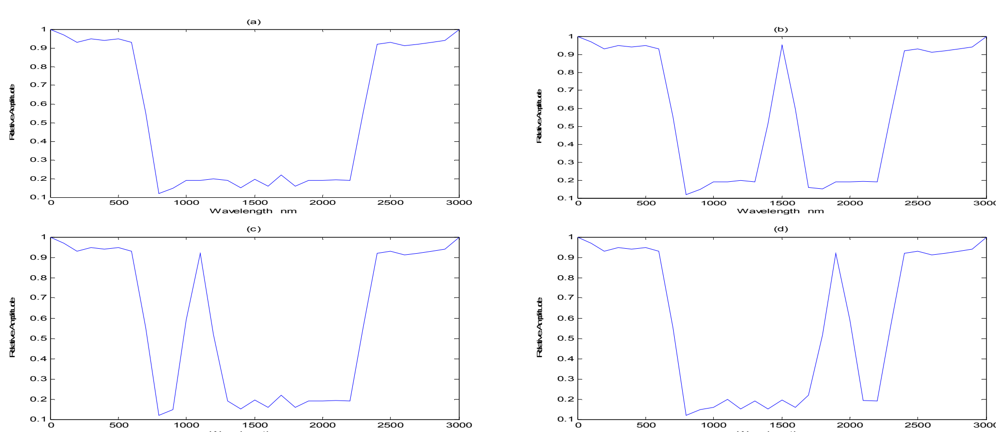

Fig 6Phase shift fiber gratings transmission spectrum (a) (b) (c) (d)

3) The principle of optical heterodyne detection

In optical heterodyne detection technology, the frequency difference ω_0 between the two beams of the laser beam until the photo detector surface, and each linear polarization output receiving optical field can be expressed as

$$\begin{cases} E_1 \exp(j\omega_1 t) \\ E_2 \exp\left[j(\omega_1 + \omega_0)t\right] \end{cases} \tag{18}$$

Where E_1 、 E_1 is Optical field intensity, ω_1 is fixed laser frequency, ω_0 is frequency difference of two lasers. Two beam are mixing frequency in the detector surface and then vector composition, the photocurrent intensity after the photoelectric conversion may be expressed as

$$I(t) = E_1^2 + E_2^2 + 2\cos\phi\left[E_1 E_2 \cos(\omega_0)t\right] \tag{19}$$

Where ϕ is angle of two-beam in the direction of polarization, photoelectric receiver frequency response is far behind optical frequency, so omit sum-frequency and one time frequency, only leave difference frequency. The photocurrent may be expressed as

$$I(t) = \left[\frac{ek}{hv}\right]\left\{E_1^2 + E_2^2 + 2F(\omega_0)\cos\phi\left[E_1 E_2 \cos(\omega_0)t\right]\right\} \tag{20}$$

Where e is electronic charge, k is quantum efficiency, hv is Photon energy, $F(\omega_0)$ is frequency response function of detector. The last type is the frequency ω_0 of the beat frequency signal. Therefore measured the beat frequency signal power by the spectrum analyzer is

$$P(\omega_0) = 2\left[\frac{ek}{hv}\right]^2 E_1^2 E_2^2 R \cos^2\phi\left[F^2(\omega_0)\right]\arctan\left(\frac{2\pi B}{\Delta\omega}\right) \tag{21}$$

Where R spectrum analyzer's input impedance, B is spectrum analyzer resolution bandwidth, $\Delta\omega$ is line width of difference frequency signal (FWHM). It is equal to the difference between the two laser line width. The typical two laser heterodyne interferometer detection system is shown in figure 7.

4) Metal fiber grating THz signal frequency detection

THz metal Fiber Grating detection uses photoelectric coherent detection, has high sensitivity. THz metal Fiber Grating frequency detection uses photoelectric heterodyne method, which uses low-loss of compensation sensor enhances the equivalent gain of the working sensor, and overcomes the effects of interference and noise. The microwave counter was already mature. This program is effective THz signal detection method. As a result of diversity reception methods and non-linear approach used in the computer signal processing, it can demodulate the weak and complex sensor information.

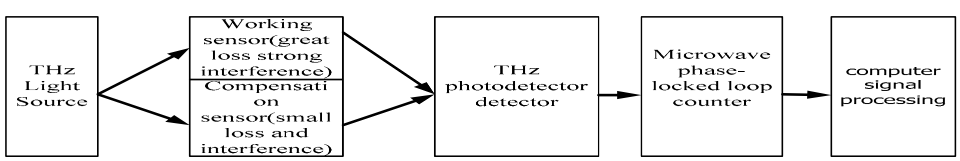

Fig 7 THz metal fiber grating signal detection and processing diagram

2.3 Down hole sensor

Take drilling sensor for an example.

THz laser issues a wide-spectrum laser, through THz transmission optical fiber and spun optical fiber joint making THz optical fiber coupled to phase shift FBG with a metal / dielectric , the reflected sensing signals through spun optical fiber joint to the photoelectric receiver for optoelectronic heterodyne, then through the electronic cable for counting processing ,non-linear signal detection, as well as diversity reception, so it is convenient to demodulate the strain and temperature information.

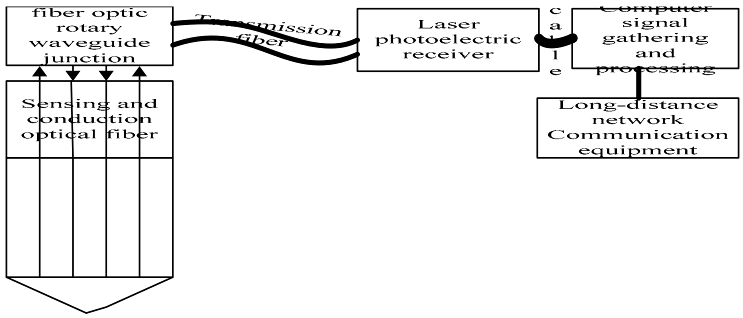

Fig 8 Metal fiber grating sensing drilling sensor diagram

3. SIMULATION AND EXPERIMENT

3.1 Experimental device

1) THz parametric oscillator (THz-TPO) which drove with the optical fiber laser measured absorption of several medium in the 200μm wave length.TPO used the optical fiber pulse laser irradiating nonlinear optical crystal in the single resonator [14], then generated THz electromagnetic wave. Pump source is Nd:YAG Q switch laser with the wavelength 1064 nm. Nonlinear optical crystal is MgO:LiNbO^3.The wavelength is between 150μm and 280μm.

By coherent detection technology, we use computer software to achieve the function of lock-in amplifier.

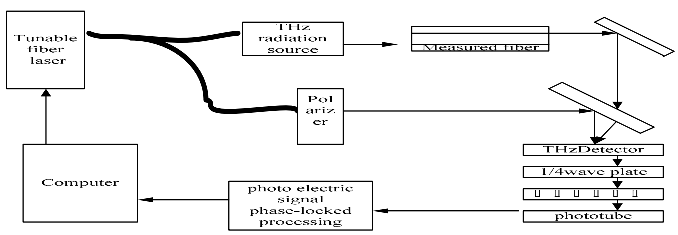

Fig 9 Dielectric-coated metal fiber detection system

After tested, the most use of the value of the model is TE11 conduction, and it is identical to other information. Showed in Figure 10 (a).

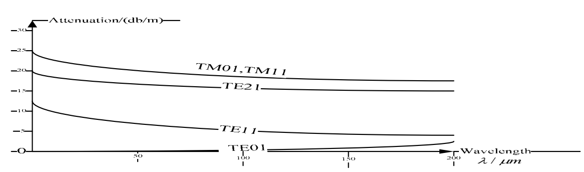

Fig. 10 (a) Dielectric-coated metal fiber detection system

Using a variety of metal did experiment to verify for film conduction mode TE11 attenuation, Ag and Al decay constant is similar to $n/\left(n^2+k^2\right)$, and it is identical to other information. Consider for technology, we used Ag.

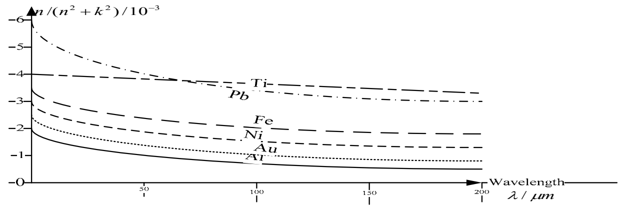

Fig. 10 (b) dielectric-coated metal fiber detection system

Consider the absorption of after polytetrafluoroethylene (PTFE) [15], polyethylene, acrylic resin ring (COP) and polycarbonate (PC) in 200μm. We can view that PE absorption is minimum in the four common dielectric materials, so it is one of the ideal combination of Ag + PE to produce dielectric-coated metal terahertz hollow optical fiber.

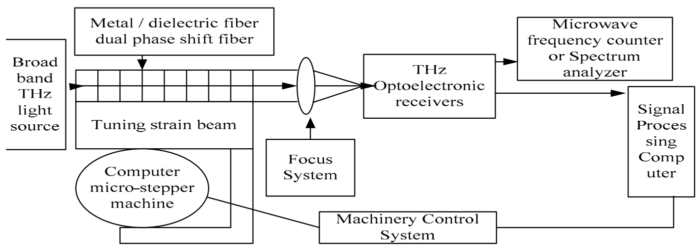

Fig 11The dual phase shift gratings difference frequency coherent detection system

The sensor output frequency May calculate based on under formula through two wavelength difference.

$$\Delta f = c[(1/\lambda_1) - (1/\lambda_2)] = c(\lambda_1 - \lambda_2)/\lambda_1\lambda_2 \approx c\Delta\lambda/\lambda^2 \qquad (3\text{-}17)$$

Where λ_1, λ_2 respectively is two grating transmission frequency, $\Delta\lambda$ is transmission frequency deviation. Δf is the band. Frequency characteristics of fiber grating figures test results are shown in Table 1.

The steps of Stepping Motor	The upper grating frequency window(nm)	The lower grating frequency window(nm)	Theoretical calculation of the difference frequency(MHz)	Measured frequency difference(MHz)
5	155000.10	154999.90	0.2500	0.2508
10	155000.15	154999.85	0.3750	0.3748
15	155000.20	154999.80	0.5000	0.5005
20	155000.26	154999.76	0.6250	0.6261
25	155000.30	154999.70	0.7500	0.7495
45	155000.35	154999.65	0.8760	0.8757
55	155000.41	154999.60	1.0125	1.0131
60	155000.44	154999.54	1.1250	1.1248

Table 1 dielectric-coated metal fiber grating sensor frequency output result

As can be seen from the table the frequency range is up to 1012Hz, the frequency resolution is 1KHz.

3.2 Signal demodulation and processing

Through electro-optical mix processing, demodulate fiber grating's complex signal. The method is showed in Figure 12.As a result of the signal nonlinear, the signal processing is very difficult, which is study key point in future.

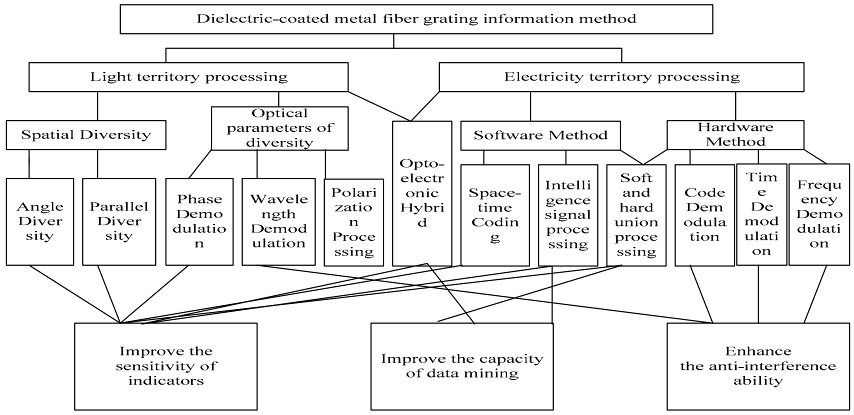

Figure 12Fiber Bragg Grating sensor Collected Annotations of the sub-frame transfer method

4. CONCLUSION

To solve the measurement problems of pressure, temperature, inclination and other important parameters underground[16], it is a satisfactory solution to use high-strength dielectric-coated metal structure THz hollow optical fiber grating sensor. Preliminary theoretical analysis and simulation and measurement results showed that polyethylene which has smaller absorption in the THz band an ideal choice wave for THz hollow fiber membrane material. The using of metal and dielectric-coated metal structure of hollow fiber graves phase shift optical fiber grating, constitutes a form of contingency temperature and pressure sensors. Differential structure can be used to overcome environmental effect. The temperature of the mine drill pipe and mine strain is detected with metal fiber. Dielectric-coated metal structure of hollow optical fiber uses coherent detection method to obtain very high gain, Phase-Shifted Fiber Grating detects frequency using optical heterodyne method, the frequency range is up to 1012Hz, the frequency resolution is 1KHz. The combination of LPFG[17], photovoltaic devices and microwave heterodyne frequency meter can resolve the problem of speed and resolution of phase-shifting grating sensor. Theoretical simulation and experimental results show that the using of dielectric-coated metal structure of hollow optical fiber enhances detection resolution four orders of magnitude, and simple structure, wide dynamic range, showing THz fiber-optic sensor technology advantages. It also has a broad application value in other harsh distributed detection environment.

REFERENCES

[1] 1 Zhang Xianbin, T. Ikari, H. Ito et al..Analysis of THz electromagnetic wave output character based on high performance 85 mm short cavity optical parametric oscillator[J].Acta Optica Sinica,2006,26(4): 616~620

[2] 2 Sun Bo, Yao Jianquan. Generation of terahertz wave based on optical methods[J].Chin. J. Lasers,2006,33(10): 1349~1359

[3] 3 Jun Yang, Shuangchen Ruan, Min Zhang. Real-time, continuous-wave terahertz imaging by a pyroelectric camera[J].Chin. Opt. Lett.,2008,6(1): 29~31

[4] 4 R. W. McGowan, G. Gallot, D. Grischkowsky. Propagation of ultrawide band short pulses of terahertz radiation through submillimeter-diameter circular waveguides [J].Opt. Lett.,1999,24(20): 1431~1433

[5] 5 G. Gallot, S. P. Jamison, D. Grischkowsky et al..Terahertz waveguides[J].J. Opt. Soc. Am. B,2000,17(5): 851~863

[6] 6 T. Hidaka, H. Minamide, S. Ichikawa et al..Ferroelectric PVDF cladding terahertz waveguide[J].J. Lightw ave Technol.,2005,23(8): 2469~2473

[7] 7 J. A. Harrington, R. George, E. Mueller et al..Hollow polycarbonate waveguides with inner Cu coatings for delivery of terahertz radiation[J].Opt. Exp.,2004,12(21): 5263~5268

[8] 8 T. Ito, Y. Matsuura, H. Ito et al..Flexible terahertz fiber optics with low bend-induced losses[J].J. Opt. Soc. Am. B,
2007,24(5): 1230~1235

[9] 9 B. Bowden, J. A. Harrington, O. Microfanov. Silver/polystyrene-coated hollow glass waveguides for the transmissionof terahertz radiation[J].Opt. Lett.,2007,32(20): 2945~2947

[10] Shu X,Zhang L,Bennion I.Sensitivity characteristics of long-period fiber gratings .J.of Lightwave Technology, 2002,20(20):255~266
[11] Ng M N,Chiang K S. Thermal effects on the transmission spectra of long-period fiber gratings. Optics Communications, 2002,208:321~327
[12] H.Ke.S.Chang,J.H.Peng.Analysis of phase-shifted long-period fiber gratings [J].IEEE Photon. Technol . Lett.,1998, 10(11):1596~1598
[13] Yokota M, Oka H.Yoshino T. Mechanically induced long-period fiber grating and its application for distributed sensing. OFS， 2002:135~138
[14] In S, Chung C, Lee H. The resonance wavelength-tuning characteristic of arc-induced by diameter modulation 15th OFS,2002,TuP2:131~ 133
[15] T.Erdogan.Cladding-mode resonance in short-and long-period fiber grating filter〔J〕.J.Opt.Soc.Am.A，1997，14(8):1760~1773
[16] C.Tsao.Optieal Fiber Waveguide Analysis〔M〕.New York: Oxford University Press，1992
[17] Xu YanPing，Gu Zhengtian，Chen Jiabi. Effect of surface film optical parameters on the eharacteristic of long-period fiber grating〔J〕.Chinese J.Laser:，2005，32(11):1519~1524